

# On the Kinetics of the Positive-Negative Temperature Dependence of Low-stress Crack Growth

A. S. KRAUSZ\* and K. KRAUSZ\*\*

*\*Department of Mechanical Engineering, University of Ottawa,  
Ottawa K1N 6N5, Canada*

*\*\*300 The Driveway, Ottawa K1S 3M6, Canada*

## ABSTRACT

Normally, the observed temperature dependence of crack growth exhibits increasing rate with increasing temperature. In the low and medium stress range of SCC (Regions I and II) the behavior was described previously by a consecutive system of two energy barriers. A synthesis method is employed to describe the anomalous behavior in which the crack growth rate shows a positive-negative temperature dependence. The synthesis model is that of two consecutive energy barriers also, with consideration of backward activation as well.

## KEYWORDS

Fracture kinetics; rate constant; forward activation; backward activation; consecutive system; energy barriers; synthesis; temperature dependence; Arrhenius plot; anomalous behavior; H<sub>2</sub> gas environment.

## INTRODUCTION

The great complexity of fracture mechanics, transport and chemical processes that are associated with subcritical environment assisted crack growth (EAC) can frustrate efforts in the analysis of the behavior that is observed in the laboratory, and at industrial and other applications. However, EAC is controlled by thermal activation; therefore, it lends itself more readily to fracture kinetics interpretation than other crack growth conditions.

A powerful tool for the furthering of the understanding of thermally activated crack growth can be found when synthesis methods are employed. The synthesis combines the fundamental principles of statistical mechanics with fracture mechanics which, drawing on basic laws, provide a solid framework: the synthesis builds models that are conclusions derived from principles. Their validity is, therefore, firmly established.

It must be made clear that developments arrived at by synthesis cannot be considered to replace analysis — they do not. Each method has its appropri-

ate role in the efforts made for the understanding of crack growth. Analysis starts with observed behavior and seeks to explain it. By doing so, it inevitably faces the fact that other models, other mechanisms, more or less related, may be discovered and may indeed replace the one proposed. This uncertainty will persist for a long time, until validity can be established by the accumulation of sufficient evidences. Because synthesis starts with basic physical principles and builds models using rigorous methods, the validity of the mechanisms so arrived at is beyond question: their usefulness, however, depends on the role they have at the actually observed conditions and on the significance of the information they can provide. In the present report we bring to attention a synthesis model of the temperature dependence of crack growth.

Experimental observations of the temperature dependence of crack velocity reveal, at least in some instances (Kerns et al., 1973; Peruz and Altstetter, 1988), the type shown in Fig. 1; related behavior in crack growth and in other stochastic processes were also observed (Johnson and Paris, 1968; Wiederhorn, 1974; Bube, 1974; Tyson, 1979; Gerberich, 1983; Moody and Gerberich, 1980). This behavior is rather interesting because it is the "common wisdom" that thermally activated processes progress faster the higher is the temperature — an expectation that follows from the consideration of the physical process itself and from the usual character of the Arrhenius plot that shows increasing crack growth rate with increasing temperature; only the details of this dependence vary (Fig. 2). The usual behavior attracts attention, as it should, because it indicates that there are factors in the process that need to be considered: its understanding can provide means to control environment assisted fracture better.

Two theories were suggested. One considers the combination of the effects of three mechanisms: (1) transport, (2) diffusion and (3) surface reaction. In the other, starting from a synthesis theory Krausz and Krausz

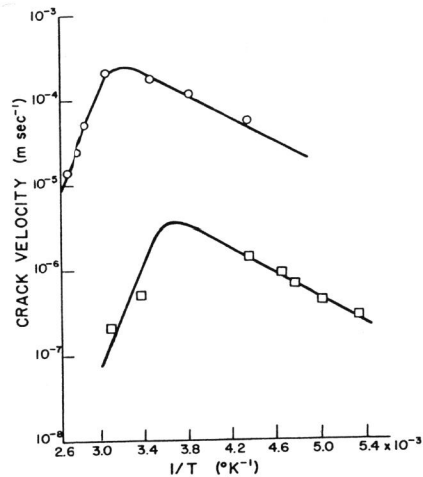


Fig. 1. The unusual Arrhenius plot measured at constant stress intensities in  $77.3 \text{ kNm}^{-2}$  hydrogen for 4130 steels of  $1330 \text{ MNm}^{-2}$  and  $1190 \text{ MNm}^{-2}$  yield strength (Kerns et al., 1973).

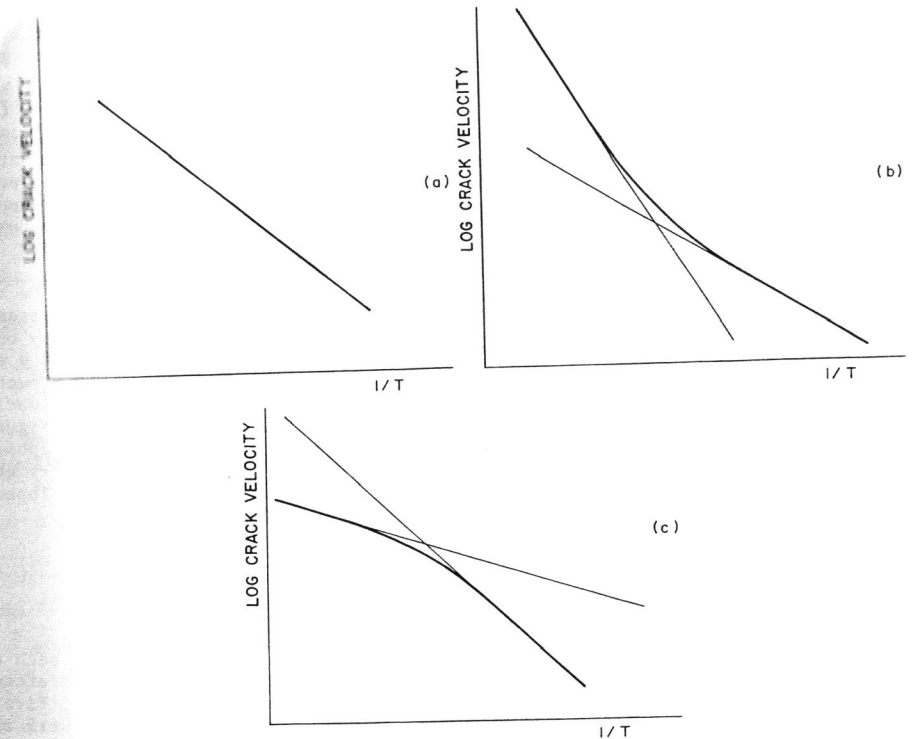


Fig. 2. Schematic representation of the Arrhenius plot for mechanisms controlled by (a) single barrier; (b) two parallel barriers; (c) two consecutive barriers. All with forward activation only.

(1988a) derived a single barrier near threshold mechanism that describes a variant of the behavior discussed in the present report. It is the purpose of this communication to report a synthesis approach derived for consecutive energy barrier kinetics from basic statistical mechanics principles that lead to the behavior shown in Fig. 1.

#### DISCUSSION

All thermally activated processes are controlled by the random fluctuation of atomic level energy contents. This common aspect of diffusion, chemical reactions, thermal conduction, plastic flow, and crack growth are at the essence of environment assisted fracture.

#### Fundamental Physical Concepts

Thermally activated processes are represented by various combinations of the elementary rate constant,  $k$ , defined by statistical mechanics as

$$k = v \exp \left[ - \frac{\Delta G^\ddagger (W)}{kT} \right] \quad (1)$$

where  $\nu$  is a frequency factor of the order of  $10^{12} \text{s}^{-1}$ ;  $\Delta G^\ddagger(W)$  is the apparent activation energy, a linear function of the true activation energy  $\Delta G^\ddagger$ ;  $W$  is the work contributed by the applied forces to crack growth;  $k$  is the Boltzmann constant; and  $T$  is the absolute temperature. Equation (1) is a somewhat simplified form to avoid carrying details of no significance for the purposes of the present synthesis. The elementary rate constant expresses the number of steps (the number of times) the crack expands per second. The apparent activation energy is defined by statistical mechanics as

$$\Delta G^\ddagger(W) = \Delta G^\ddagger - W; \quad (2)$$

in which  $\Delta G^\ddagger$  is the energy needed to make the crack grow at absolute zero when no thermal energy is available: it is the energy needed to rearrange the atoms into the configuration that exists after the crack moved by one step. This model clearly recognizes that the actual material is not a continuum but a discrete system of atoms and, correspondingly, crack growth in all materials is always a discrete, stepwise process. The true activation energy,  $\Delta G$ , is a function of the composition and of the atomic configuration: it is microstructure dependent. The mechanical energy,  $W$ , depends on the applied load, the geometry of the specimen or component (boundary conditions) and on the microstructure as well. These concepts were developed in detail recently (Krausz and Krausz, 1988b).

The crack velocity is then expressed as

$$v = \kappa k = \kappa \nu \exp \left| - \frac{\Delta G^\ddagger(W)}{kT} \right| \quad (3)$$

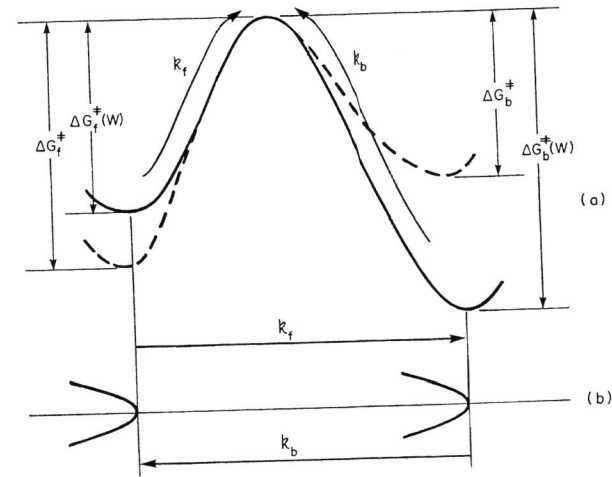
where  $\kappa$ , for the present purposes, expresses the contribution of each activation step to the crack size growth and other factors such as the effect of the concentration of the degrading environmental species. As a first approximation  $\kappa$  is considered to be independent of the applied work and the temperature: this will be discussed later. Fig. 2(a) is the typical Arrhenius representation of eq. (3) at constant work and microstructure.

It is customary for visualization purposes to represent the energy barrier associated with the rate constant,  $k$ , as shown in Fig. 3. In the model it is recognized that, as the fundamental principle of statistical mechanics, all thermally activated processes occur in the "backward" as well as in the "forward" direction; in the case of crack growth, these are equivalent to atomic bond breaking when the crack grows by one step, and to atomic bond healing by which the crack shrinks by one step at the corresponding activation event. The subscripts represent these by  $f$  for forward (breaking) and  $b$  for backward (healing) event. The appropriate directions for the movement over the energy barrier are shown by the arrows. These principles state that equilibrium is always a dynamic state at the submicrostructural level: there is a very frequent fluctuation over the energy barrier at the rates

$$\kappa_f k_f = \kappa_b k_b \quad (4)$$

so that at the macroscopic level no crack size change is observed. This state follows from the definition of the two rate constants

$$k_f = \nu \exp \left| - \frac{\Delta G_f^\ddagger(W_f)}{kT} \right| = \nu \exp \left( - \frac{\Delta G_f^\ddagger - W_f}{kT} \right)$$



- (a). The energy barrier. The height of the energy barrier in the absence of mechanical energy is  $\Delta G^\ddagger$ ; when work is applied it changes to  $\Delta G^\ddagger(W) = \Delta G^\ddagger - W$ . This is shown by the change from the dashed line form to that of the solid line.
- (b). The locations of the crack tip and their activation direction shown by the arrows and identified by the rate constants defined in the text.

$$k_b = \nu \exp \left| - \frac{\Delta G_b^\ddagger(W_b)}{kT} \right| = \nu \exp \left( - \frac{\Delta G_b^\ddagger + W_b}{kT} \right). \quad (5)$$

Equilibrium is when

$$\kappa_f \nu \exp \left| - \frac{\Delta G_f^\ddagger(W_f)}{kT} \right| = \kappa_b \nu \exp \left| - \frac{\Delta G_b^\ddagger(W_b)}{kT} \right|. \quad (6)$$

When the work is greater than what produces equilibrium  $k_f > k_b$ , and the crack grows. These conditions are quite general and apply to any material when fracture occurs by thermal activation.

In general, there are several processes associated with crack growth: environment assisted fracture is a particularly complex combination. Order is brought into this complexity by fracture kinetics theory. The theory shows (Krausz and Krausz, 1988b); Krausz and Eyring, 1975) that all combinations (that are of first order kinetics) are either parallel or consecutive combinations of energy barriers; or, in the most general case, a sum of these two. The corresponding Arrhenius plots are shown in Fig. 2. Fracture kinetics expresses their rate equations by the appropriate combination of elementary rate constants

$$v = f(k_i). \quad (7)$$

These combinations are derived rigorously from statistical mechanics principles; they are firmly established integral parts of the kinetics theory of all thermally activated processes (Krausz and Krausz, 1988b; Krausz and Eyring, 1975; Glasstone et al., 1941; Benson, 1960).

### The Kinetics Model

It is well established that Regions I and II of stress corrosion cracking (SCC) are described by a consecutive system of two energy barriers. It is proposed that the same model can be used to describe the experimental results shown in Fig. 4, leading to the description of the "unconventional" temperature dependence shown in Fig. 1.

A consecutive energy barrier system consisting of two components is shown schematically in Fig. 5. The arrows indicate the elementary rate constants, the subscripts identify the direction of the thermally activated step and the barrier with which the elementary rate constant is associated. This character of the energy barrier system exists in a range of applied mechanical energy,  $W$ , and is the essential state of the investigated mechanism. As we discussed before

$$\Delta G^\dagger(W) = \Delta G^\dagger - W, \quad (8)$$

where  $\Delta G^\dagger$  is the free energy of activation and  $W$  is the function of an appropriate fracture mechanics quantity,  $K$ ,  $\Delta K$ ,  $J$ -integral, COD, etc.; for instance

$$W = \alpha K \quad (9)$$

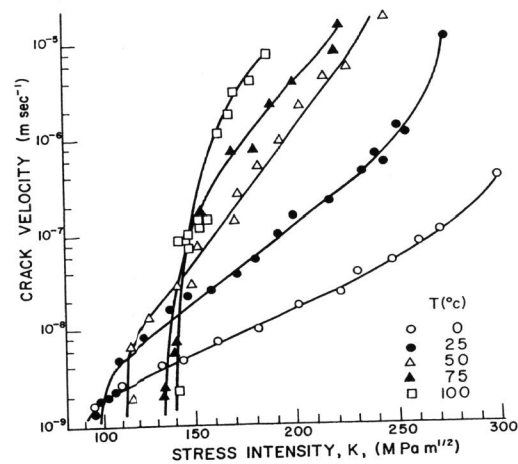


Fig. 4. Measured behavior in a stainless steel (~50 pct. austenite in a ferritic matrix) tested in  $H_2$  gas at 108 kPa (Peruz and Altstetter, 1988).

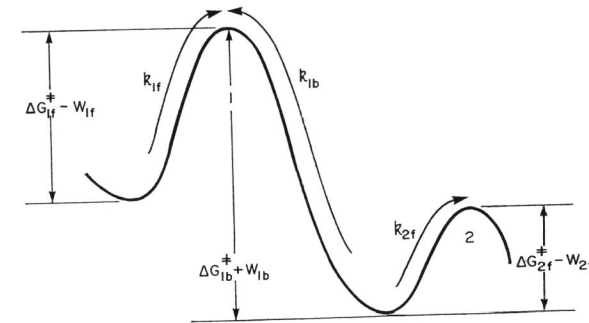


Fig. 5. A system of two consecutive energy barriers.

where  $\alpha$  is the work factor that depends on the mechanism of the crack growth process and on the microstructure. Accordingly,

$$\begin{aligned} k_{f1} &= v \exp \left| - \frac{\Delta G_{f1}^\dagger(W)}{kT} \right|, \\ k_{f2} &= v \exp \left| - \frac{\Delta G_{f2}^\dagger(W)}{kT} \right|, \\ k_{b1} &= v \exp \left| - \frac{\Delta G_{b1}^\dagger(W)}{kT} \right|. \end{aligned} \quad (10)$$

It was shown (Krausz and Krausz, 1988b) that the crack velocity,  $v$ , over a two-barrier system is described by the constitutive equation as

$$v = \frac{\kappa_{f1} k_{f1} \kappa_{f2} k_{f2}}{\kappa_{f1} k_{f1} + \kappa_{b1} k_{b1}} \quad (11)$$

where  $\kappa$  is the function of environmental gas pressure, concentration, crack growth step, etc. Substitution of eqs. (10) and (11) results in

$$v = v \frac{\kappa_{f1} \kappa_{f2} \exp \left| - \frac{\Delta G_{f1}^\dagger(W) + \Delta G_{f2}^\dagger(W)}{kT} \right|}{\kappa_{f1} \exp \left| - \frac{\Delta G_{f1}^\dagger(W)}{kT} \right| + \kappa_{b1} \exp \left| - \frac{\Delta G_{b1}^\dagger(W)}{kT} \right|} \quad (12)$$

The relation of the two terms in the denominator can be appreciated from Fig. 6, where  $\log \kappa_{f1} k_{f1}$  and  $\log \kappa_{b1} k_{b1}$  are represented as a function of  $1/T$ . The slope of the lines is  $\Delta G^\dagger(W)/k$  and the intercept at  $1/T = 0$  is  $v\kappa$ . Clearly, where  $\kappa_{b1} k_{b1} \gg \kappa_{f1} k_{f1}$ , the greater one dominates; alternatively, at high  $1/T$ ,  $\kappa_{f1} k_{f1}$  is greater and the effect of  $\kappa_{b1} k_{b1}$  is negligible; where both are about the same magnitude the behavior is along the curved segment. The heavy line indicates the macroscopically, experimentally observable effect. In short, at high temperatures  $\kappa_{b1} k_{b1}$  controls crack growth; in the low temperature region crack growth is controlled by  $\kappa_{f1} k_{f1}$ .

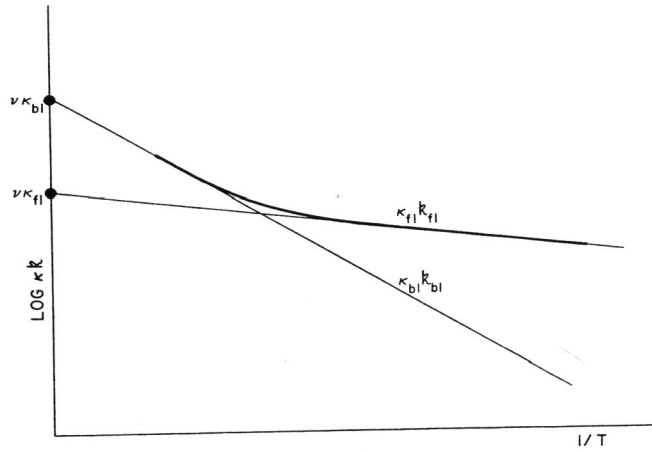


Fig. 6. Schematic representation of  $\kappa_{f1}k_{f1}$  and  $\kappa_{b1}k_{b1}$ .

Consider now the Arrhenius plot of the investigated "unconventional" behavior represented in Fig. 7, where the three regions appear in the following manner.

Region (1): high temperature region. Here  $\kappa_{b1}k_{b1} \gg \kappa_{f1}k_{f1}$ ; it follows from eq. (12) that

$$v = v \frac{\kappa_{f1}k_{f1} \kappa_{f2}k_{f2}}{\kappa_{b1}k_{b1}} \exp \left| - \frac{\Delta G_{f1}^{\dagger}(W) + \Delta G_{f2}^{\dagger}(W) - \Delta G_{b1}^{\dagger}(W)}{kT} \right|. \quad (13)$$

Visual inspection of Fig. 5 shows that  $\Delta G_{f1}^{\dagger}(W) + \Delta G_{f2}^{\dagger}(W) < \Delta G_{b1}^{\dagger}(W)$ ; hence the exponent of eq. (13) is positive. Writing

$$- \Delta G_{f1}^{\dagger}(W) + \Delta G_{f2}^{\dagger}(W) + \Delta G_{b1}^{\dagger}(W) = \Delta G_{R1}^{\dagger}(W) \quad (14)$$

for Region 1, the crack velocity is

$$v_{R1} = v \frac{\kappa_{f1}k_{f2}}{\kappa_{b1}} \exp \left| \frac{\Delta G_{R1}^{\dagger}(W)}{kT} \right|. \quad (15)$$

That is, the slope of the  $\ln v$  vs.  $1/T$  plot is positive, as shown in Fig. 7, and is equal to  $\Delta G_{R1}^{\dagger}(W)/k$ .

Region (3): low temperature region. In this region  $\kappa_{f1}k_{f1} \gg \kappa_{b1}k_{b1}$ , hence

$$v_{R3} = v \kappa_{f2}k_{f2} = v \kappa_{f2} \exp \left| - \frac{\Delta G_{f2}^{\dagger}(W)}{kT} \right| \quad (16)$$

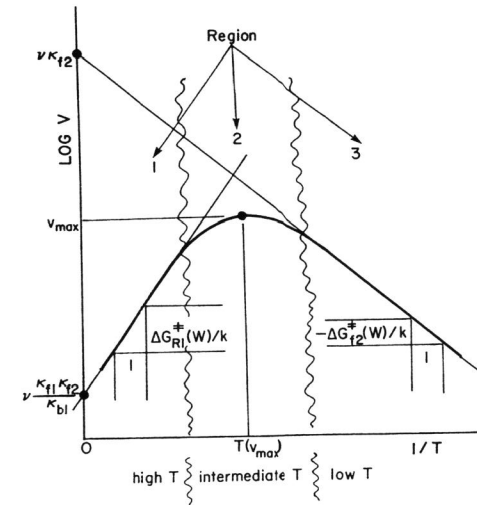


Fig. 7. Schematic representation of the temperature dependence of the crack velocity in the three temperature regions. The crack velocity is described in Region 1 by  $v_{R1}$ ; in Region 2 by eq. (12), and in Region 3 by  $v_{R3}$ .

and, therefore, the slope of the  $\ln v$  vs.  $1/T$  plot is negative and is equal to  $-\Delta G_{f2}^{\dagger}(W)/k$ , as shown on the right hand side of Fig. 7.

Region 2: intermediate temperature region. In this region  $\kappa_{f1}k_{f1} \approx \kappa_{b1}k_{b1}$  and, therefore, the full expression of the constitutive equation (12) describes the temperature dependence of the crack velocity. The consequence is that in this region the  $\ln v$  vs.  $1/T$  relation is a curve (Fig. 7), while in the other two regions straight lines (corresponding to single exponential expressions) represent the behavior.

It follows from the analysis that  $\kappa_{f2} \gg \kappa_{f1}k_{f2}/\kappa_{b1}$ , as demonstrated in Fig. 7; hence  $\kappa_{b1} \gg \kappa_{f1}$ . The maximum velocity is where  $v(R1) = v(R3)$

$$v_{\max} = v \frac{\kappa_{f1}}{\kappa_{b1}} \exp \left| \frac{\Delta G_{R1}^{\dagger}(W)}{kT} \right| = v \kappa_{f2} \exp \left| - \frac{\Delta G_{f2}^{\dagger}(W)}{kT} \right|. \quad (17)$$

and the temperature at which  $v$  is maximum is

$$T(v_{\max}) = \frac{\Delta G_{R1}^{\dagger}(W) + \Delta G_{f2}^{\dagger}(W)}{k \ln \kappa_{b1}/\kappa_{f1}}. \quad (18)$$

Fig. 8(a) shows the behavior in the  $\log v$  vs. crack driving force (here as  $k$ ) coordinate system; the corresponding  $\log v$  vs.  $1/T$  system is shown in Fig. 8(b). The two figures are coordinated in the sense that one can be constructed from the other by keeping the scales identical. These illus-

trate, and prove by geometrical argument the completeness of the theory. Comparison with the experimentally observed behavior (Figs. 1 and 4) is illuminating. Similar agreements are found with other measured results (Sawicki, 1973).

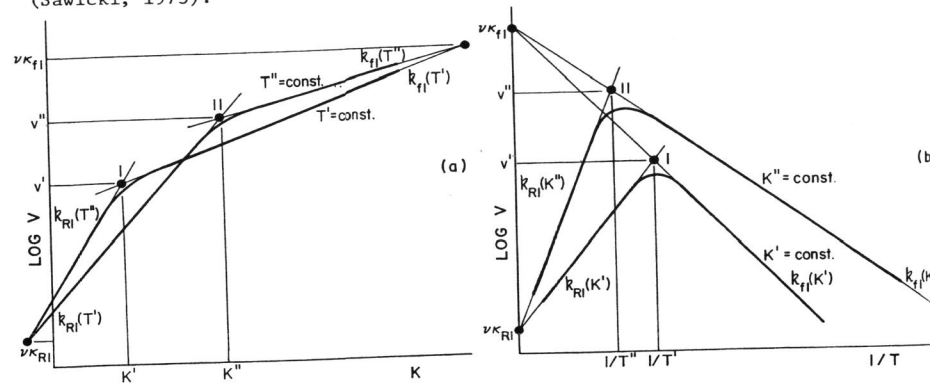


Fig. 8. The schematic representation of crack growth behavior showing the coordination of the two systems of variables.

- (a) The crack growth behavior as the function of the stress intensity factor at two temperature levels.
- (b) The crack growth behavior as the function of the temperature at two constant stress intensity factor levels. The intersections identified as ● correspond to the same K, T, and v each, and are the same as in Fig. 8(a).

- Benson, S.W. (1960). The Foundations of Chemical Kinetics. McGraw-Hill, New York.
- Bube, R.H. (1974). Electronic Properties of Crystalline Solids. Academic Press.
- Gerberich, W.W. (1983). (communication at a workshop on "Media with Micro-Structure", Michigan Technological University).
- Glasstone, S., K.J. Laidler and H. Eyring (1941). The Theory of Rate Processes. McGraw-Hill, New York.
- Johnson, H.H. and P.C. Paris (1968). Subcritical Flaw Growth. Engineering Fracture Mechanics, 1, 3-45.
- Kerns, G.E., M.T. Wang and R.W. Staehle (1973). In: Stress Corrosion Cracking and Hydrogen Embrittlement of Iron Base Alloys. National Assoc. Corrosion Engineers, 5, 700-735.
- Krausz, A.S. and H. Eyring (1975). Deformation Kinetics. Wiley Interscience, New York.
- Krausz, A.S. and K. Krausz (1988a). In: Materials Engineering for High Risk Environment. Proceedings of NUCMAT-88 (A. Niku-Lari Ed.) 1-11.
- Krausz, A.S. and K. Krausz (1988b). Fracture Kinetics of Crack Growth. Kluwer Academic Publishers, Dordrecht.
- Moody, N.R. and W.W. Gerberich (1980). Hydrogen Induced Slow Crack Growth in Ti-6Al-6V-2Sn. Metallurgical Transactions, 11A, 973-981.
- Peruz, T.-P. and C.J. Altstetter (1988). Cracking Kinetics of Two-phase Stainless Steel Alloys in Hydrogen Gas. Metallurgical Transactions, 19A, 145-152.
- Sawicki, V.R. Jr. (1973). In: Stress Corrosion Cracking and Hydrogen Embrittlement of Iron Base Alloys. National Assoc. Corrosion Engineers, 5, p.719 and p. 725.
- Tyson, W. (1979). Hydrogen in Metals. Canadian Metallurgical Quarterly, 18, 1-11.
- Wiederhorn, S.W. (1974). Subcritical Crack Growth in Ceramics. In: Fracture Mechanics of Ceramics, (Ed. R.C. Bradt, D.P.H. Hasselman and F.T. Lange), 2, 613-646, Plenum Press.